To what Extent Can Vegetation Mitigate Greenhouse Warming? A Modeling Approach

L. Bounoua[1]*, F. G. Hall[2], P. J. Sellers[3], A. Kumar[4], G. J. Collatz[1], C. J Tucker[1]

Abstract

Climate models participating in the IPCC Fourth Assessment Report indicate that under a $2xCO_2$ environment, runoff would increase faster than precipitation overland. However, observations over large U.S watersheds indicate otherwise. This inconsistency suggests that there may be important feedbacks between climate and land surface unaccounted for in the present generation of models. We postulate that the increase in precipitation associated with the increase in CO_2 is also increasing vegetation density, which may already be feeding back onto climate. Including this feedback in a climate model simulation resulted in precipitation and runoff trends consistent with observations and reduced the warming by 0.6°C overland. This unaccounted for missing water may be linked to about 10% of the missing land carbon sink.

A recent compilation of outputs from 19 coupled atmosphere-ocean general circulation models used in the IPCC Fourth Assessment Report (AR4) shows projected increases in air temperature, precipitation and river discharge for 24 major rivers in the

[1]* L. Bounoua NASA GSFC, Code 614.4, Greenbelt, MD 20771
[2] F. G. Hall UMBC and GSFC, Code 614.4, Greenbelt, MD 20771
[3] P. J. Sellers NASA JSC, Code CB, Houston, TX 77058
[4] A. Kumar NOAA CPC, Camp Springs, MD 20746
[1] G. J. Collatz NASA GSFC, Code 614.4, Greenbelt, MD 20771
[1] C. J. Tucker NASA GSFC, Code 614.4, Greenbelt, MD 20771

world in response to doubling CO_2 by the end of the century (1). The ensemble mean from these models also indicates that, compared to their respective baselines overland, the global mean of the runoff change would increase faster (8.9% per year) than that of the precipitation (5% per year).

We analyze century-scale observed annual runoff time-series (1901-2002) over 9 hydrological units covering large regions of the Eastern United States (Fig.1) compiled by the United States Geological Survey (USGS)(2). These regions were selected because they are the most forested; the least water-limited and are not under extensive irrigation. We compare these time-series to similar time-series of observed annual precipitation anomalies spanning the period 1900-1995 (3). Both time-series exhibit a positive long-term trend (Fig. 2); however, in contrast to the analysis of (1), these historic data records show that the rate of precipitation increase is 5.5 % per year, roughly double the rate of runoff increase of 3.1% per year.

The divergence between the IPCC model simulations (1) and observations raise two important issues: 1) the disagreement suggests that there may be important feedback processes between the climate and land surface unaccounted for in the models. 2) The fact that there is a widening difference between observed precipitation and runoff trends raises the question, where is the excess water going? That is, where is the missing water? Is it stored in surface reservoirs for irrigation and human use; is it going to recharge aquifers; is it utilized by natural vegetation; or all of the above?

We considered all these possibilities (supporting online material S1) and concluded that none of these processes acting alone could account for the total excess water generated by the observed difference between precipitation and runoff. We hypothesize then that in water-limited conditions, the additional water available from increasing precipitation stimulates vegetation growth; hence increases evapotranspiration rates, thus reducing the rate of increase in runoff. This feedback, not incorporated in the IPCC models used by (1), has important implications for climate and the carbon budget. We show that in a doubled-CO_2 atmosphere, this feedback: 1) slows atmospheric warming by accelerating the recycling of water between the land and atmosphere, and 2) steadily increases the land carbon sink through an increase in terrestrial vegetation biomass.

In the supporting online material, S1, we show that the excess water resulting from the increasing difference between precipitation and runoff must also result in increasing evapotranspiration. We also show that the NDVI is significantly correlated with the precipitation minus runoff difference. This is consistent with the hypothesis that part of the excess water is favoring an increase in vegetation growth with an associated increase in evapotranspiration. We investigated the implication of this important feedback for the projected changes in precipitation, air temperature, runoff and carbon uptake as well as their consistency with the observed trends. We used a version of the Colorado State University (CSU) coupled land surface ocean climate model (4) with the Simple Biosphere model (SiB2) of (5,6) used for land surface vegetation and carbon exchanges. We compared three plausible future vegetation-climate interaction scenarios, two of which build on our previous work (7,8). The first scenario was a conventional 2xCO_2

simulation (**CV**) in which both the radiative forcing and the vegetation physiology operate under a $2xCO_2$ environment, 700 ppm. In the second scenario, we investigated the effect of vegetation physiological down-regulation on the surface water, energy and carbon budgets under a $2xCO_2$ concentration. Down-regulation (**DR**) was prescribed in the doubled CO_2 environment by requiring the physiological model to maintain carbon assimilation rates consistent with a $1xCO_2$ (350 ppm) atmosphere (7) which leads to an increase in the vegetation's water use efficiency (WUE) and a relative decrease in evapotranspiration, (WUE is the ratio of carbon assimilated to the amount of water transpired by vegetation). Since the study of (7) others have examined the effect of this physiological down-regulation on the hydrological cycle and have reported similar results (9,10). In the third scenario labeled (**IB**), we examined the effect of our hypothesized vegetation response to increased CO_2 and water availability. The IB simulation was identical to the DR simulation except that vegetation leaf density was allowed to increase to take advantage of the increased CO_2 where water is not limiting evapotranspiration (supporting online material S2). In other words, during the IB-simulation the global canopy net photosynthesis rate with down-regulation should approach that of the unadjusted CV-case. This was achieved by allowing leaf density to increase and compensate for the DR stomatal closure effect. In SiB2, an increase in leaf density not only affects the carbon uptake, the transpiration and interception rates, but it also alters the surface albedo and roughness length and so affects the turbulent exchange of energy, water and momentum at the land-atmosphere interface. These three simulations CV, DR and IB (11) were compared to a control simulation (**C**) using 350 ppm for both the radiative and physiological modules of the coupled climate model.

The globally-averaged precipitation over the last 10 years of the control simulation was 2.88 $mm.day^{-1}$ slightly greater than the observed 2.74 $mm.day^{-1}$, from the Global Precipitation Climatology Project figure, reported in (1).

The introduction of the additional vegetation-climate feedback (IB-case) had an important impact on the hydrological cycle (Table 1). In sharp contrast to results from (1) and to our own CV and DR-cases results, when the increase in vegetation density (IB-case) feedback was introduced, the global trend in runoff (4.0%) was smaller than that of precipitation (4.3%), similar to the observed trends over the large Eastern U.S watersheds (Fig.2). Over the Eastern United States (Fig.1), the IB-case modeled precipitation increase (35.7 %) is larger than increase in runoff (34.6 %), consistent with the observed trends (Table 1.b). The IB-results are also in line with those from (12) which show decreases in stream flow following the first couple of years of forest growth. Similar to the IPCC results of (1), in the CV case the relative increase in runoff is larger than that of precipitation. These trends are even more amplified in the DR-case where the runoff increased by 6.7 % and the precipitation increased only by 3%. These results suggest that: 1) the IB-scenario is more realistic than the CV and DR cases and, 2) the results from the IPCC models used in (1) simulate the doubling of CO_2 along a line between the CV and DR-cases.

The vegetation-climate feedback introduced in the IB-case also had significant implications for the energy cycle. Globally, the CV-case increase in surface temperature was 1.9 °C, in the lower end of the 2.0 to 4.5 °C range projected by the IPCC

for the global warming following an equilibrium doubling of CO_2 (13). In the IB-case, however, the projected global temperature increase is only 1.7 °C (Table 2b) suggesting that the additional vegetation climate feedback has reduced the warming globally by about 0.3 °C compared to the conventional case (CV). This global surface temperature warming is about 1.3 °C less than the IPCC best estimate of 3 °C (13). Over land the results are striking, the IB-case surface temperature increased only 2.2 °C over the control; that is a marked cooling of about 0.6 °C compared to the CV-case and 0.4 °C below the DR-case. Over the Eastern USA regions (Fig.1), the increase in vegetation has dramatically reduced the warming to about 1.5 °C cooler than the conventional CV-case.

Under the IB scenario, the model simulated a carbon uptake increase of 44.45 $PgC.yr^{-1}$ for a 350 ppm CO_2 increase (Table 2a). Is this increase consistent with observed increase in the land carbon sink, which shows an acceleration of 0.036 $PgC.yr^{-2}$ (14) from 1960 to 2000? For the 50 ppm CO_2 increase observed from 1960 to 2000 (14), the model would project an annual increase in carbon uptake of 0.16 $PgC.yr^{-2}$. However, only about 2% of the current global carbon uptake is sequestrated on land and about 98% of it is returned to the atmosphere via heterotrophic respiration (15); hence for the 1960 to 2000 period, the model projects a land carbon sink accelerating at 0.0032 $PgC.yr^{-2}$, about a tenth of the magnitude of the observed increase. Thus, increased land carbon sequestration resulting from CO_2 fertilization and increased precipitation projected by the coupled model, while consistent with the observed increase in the land carbon sink and well within the constraints of the nitrogen availability reported in (16), can explain about 10% of it; the

remainder likely resulting from biomass recovery following disturbance, shrub encroachment or other mechanisms discussed in (17).

The results discussed here do not address other changes in the terrestrial carbon cycle that may take place in a warming climate; for example, an increase in the growing season which may lead to results similar to ours or the warming and drying of the northern tundra and boreal forest regions, which may result in large-scale releases of CO_2 from terrestrial carbon stores into the atmosphere. Further work must be done with more comprehensive biosphere-atmosphere models to gain a complete picture of possible future carbon and water dynamics over the continents. However, the results presented here indicate that changes in the state of vegetation may already be playing a role in the continental water, energy and carbon budgets as atmospheric CO_2 increases.

References

1. D. Nohara, A. Kitoh, M. Hosaka, T. Oki, *J. Hydrometeorol.*, **7** (2006).
2. U. S. Geological Survey, data available at http://water.usgs.gov/waterwatch/
3. A. Dai., I.Y. Fung, A.D. Del Genio. *J. Climate* **10** (1997).
4. D. A. Randall et al, *J. Climate*, **9**, 738 (1996).
5. P. J. Sellers et al, *J. Climate*, **9**, 676 (1996)
6. P.J. Sellers et al, *Science*, **275**, 502, (1997).
7. P.J. Sellers et al, *Science*, **271**, 1402, (1996).
8. L. Bounoua et al, *J. Climate*, **12**, 309 (1999).
9. N. Gedney et al, Nature **439**, 835 (2006).

10. R. A. Betts et al, Nature **448**, 1037 (2007).

11. All simulations are started from the same initial conditions obtained from a 20- year spin up run and carried out 30 years. Simulations are run at 7.2 ^{o} x 9.0^{o} horizontal resolution and 9 vertical layers.

12. R. B. Jackson et al, *Science*, **310**, 1944 (2005).

13. Intergovernmental Panel on Climate Change, Climate Change: The Physical Science basis. Contribution of Working Group I to the Fourth Assessment Report of the Intergovernmental Panel On Climate Change, (2007).

14. Global carbon budget; data available at http://lgmacweb.env.uea.ac.uk/lequere/co2/carbon_budget.htm

15. Schlesinger, William H., 1991: Biogeochemistry: An Analysis of Global Change. Academic Press. 443 pp.

16. B. A. Hungate et al, *Science*, **302**, 1512, (2003).

17. Pacala SW et al, Science, **292**, 2316, (2001).

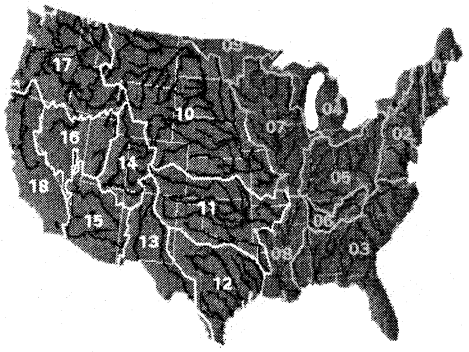

Figure 1. Area highlighted green is where observational analyses were performed. The area consists of 9 hydrological units as defined by USGS(3).

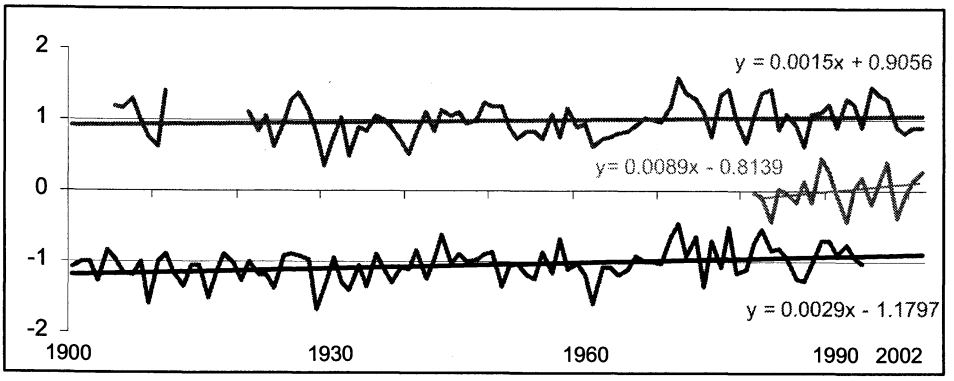

Figure 2: Annual runoff (Red) (1901-2002), precipitation (Blue) (1901-1995) and NDVI (green) (1982-2002) anomalies for the study area highlighted green in Figure 1. An offset of +1/-1 is added to runoff and precipitation, respectively for plotting purpose. Periods with no available data are left blank. Note that the slope of the precipitation regression line is about twice that of runoff.

A: Precipitation

	C	CV-C	DR-C	IB-C
Global	2.88	4.7 (0.135)	3.9 (0.11)	4.2 (0.120)
Land	2.75	6.4 (0.175)	3.0 (0.083)	4.3 (0.119)
East. US	2.36	31.2 (0.735)	10.4 (0.246)	35.7 (0.843)

B: Runoff

	C	CV-C	DR-C	IB-C
Global				
Land	1.15	9.8 (0.113)	6.7 (0.077)	4.0 (0.046)
Eastern. US	1.60	35.4 (0.567)	10.9 (0.174)	34.6 (0.554)

Table 1: Control values and relative changes from to the control values in percent for (A) precipitation in $mm.day^{-1}$ and (B) runoff in $mm.day^{-1}$. Values in parenthesis are absolute difference from the control. Observed relative changes for the Eastern US regions are 5.5% for precipitation and 3.1% for runoff. Eastern U.S. corresponds to the area highlighted green in Figure 1. All values are obtained as averages over the last 10 years of simulations. For observed precipitation and runoff relative changes are computed using the first and last 10 years of observations.

A: Carbon Uptake

	C	CV-C	DR-C	IB-C
Global				
Land	124.80	44.60	13.43	44.45
East. US	7.23	3.13	1.32	3.92

B: Temperature

	C	CV-C	DR-C	IB-C
Global	18.53	1.94	1.84	1.68
Land	19.55	2.80	2.67	2.23
East. US	19.93	2.92	2.67	1.38

Table 2: Control and change from the control for (A) carbon uptake in Petagrams (10^{15} grams) and (B) surface temperature in Celsius.

Supplement S1

The Missing Water

Over a contained hydrological basin where continuity equations apply, the precipitation influx, P, is partitioned into evaporation, E; runoff, Ro; or contributes to changes in surface and aquifer storage, dSo/dt and dAq/dt, respectively,

$$P = E + Ro + dSo/dt + dAq/dt$$

At decadal to longer time scales, an increasing trend in basin total precipitation must therefore be balanced by the net differences in the evaporation, runoff and storage trends. As our analysis shows, observed precipitation is increasing over time at nearly twice the rate of runoff. Where is the missing water going? Is it stored in surface reservoirs for

irrigation and human use; is it going to recharge aquifers; is it utilized by natural vegetation; or all of the above?

Increasing storage in surface reservoirs?

We considered this explanation, but concluded that only a steady increase in water storage in newly constructed impoundments, dSo/dt, could explain the increasing trend in precipitation minus runoff since the steady increase in observed runoff (Fig. 2) implies that storage in existing surface reservoirs is already saturated. We estimated the total amount of water produced by the observed difference between precipitation and runoff over the study area and over time. We found that if we attribute all the change to surface storage, dSo/dt, it would cover the entire study area (Fig.1) to a depth of 3.06 meters. Since this is obviously not the case, we conclude that the difference between the precipitation and runoff trends could not be explained only by increasing storage in surface reservoirs.

Aquifers Recharge?

Our analysis shows that aquifer recharge is much smaller than precipitation minus runoff. Records of aquifer recharge rates for the 9 hydrological units in the forested study regions of Figure 1 are not available. However, we obtain an upper bound using USGS statistics on water withdrawal rates (1). Annual withdrawals, particularly in western aquifers, exceed natural recharge rates (2). Estimates indicate that after continual increases in the nation's water withdrawals from the beginning of the century,

withdrawals declined from 1980 to 1995. By 1995, ground water withdrawals declined by 4% compared to 1990 (3). To further ensure an upper bound for aquifer withdrawal rates, we use as an estimate for 1900-1995, the recorded USGS withdrawal rate for 1985, one of the highest withdrawal rates for the period 1950–1995 (3). Based on this maximum rate, we estimate the maximum amount of water withdrawn from all aquifers over the study area since the beginning of our records (1900) to be about 0.60 meters in depth. Even if this entire withdrawn amount is restored as storage, it would represent only 19.6% of the 3.06 meters total amount of water produced by the observed difference between precipitation and runoff over the study area over the same period. It is thus reasonable to conclude that the observed difference between the precipitation and runoff trends cannot be explained only by recharge to aquifers; hence evapotranspiration must also increase.

Finally, we examined to what extent increases in evapotranspiration could be explained by increases in natural vegetation density.

Increases in natural vegetation density?

Fig. S1 shows some evidence for an increase in vegetation density over the past 20 years based on the longest available global time series of AVHRR-observed Normalized Difference Vegetation Index-NDVI (4) where we plot observed precipitation minus runoff versus NDVI anomalies averaged over all the hydrological basins examined in Fig. 1. Although the R^2 (0.33) is small, partly because NDVI responds only to increase in

transpiration, it is statistically significant (p=0.034). Given the length of the NDVI time series however, we take this result as weak but significant evidence for the hypothesis that vegetation density is responding to the increased availability of soil moisture and CO_2. The fact that only 33% of the variance in vegetation density is explained by change in precipitation minus runoff suggests that the observed excess water can not be accounted for by increased vegetation density alone and that it is likely depleted between increases in vegetation evapotranspiration, soil evaporation, surface storage and aquifer recharge.

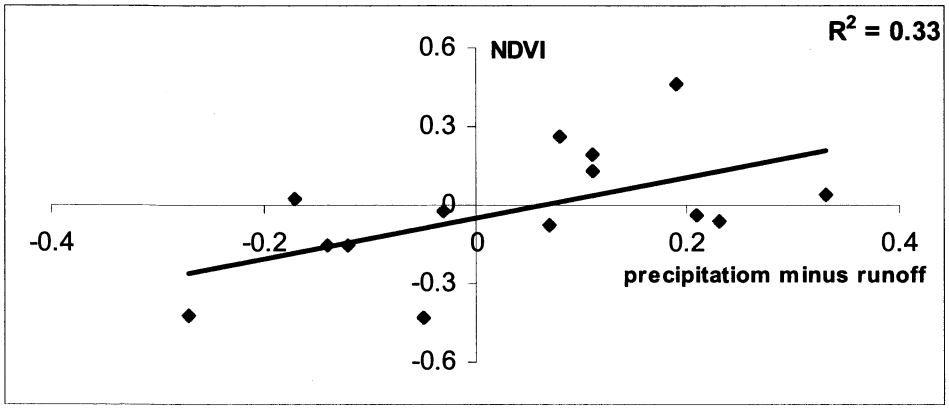

Figure S1: NDVI versus (precipitation – runoff) anomalies averaged over the 9 hydrological units highlighted green in Figure 1.

References

1 U.S. Geological Survey, Ground Water Atlas of the United States. Introduction and National Summary, James Miller (1999). Available online at http://capp.water.usgs.gov/gwa/ch_a/index.html

2 Tietenberg, T. Replenishable but Depletable Resources: Water. *In Environmental and Natural Resource Economics* (Third Edition). New York: Harper Collins: p. 222-235, (1992).

3 Solley, W. B., R. R. Pierce, and H. A. Perlman, *Estimated Use of Water in the United States in 1995.* U.S. Geological Survey Circular 1200, (1998).

4 C. J. Tucker et al, *Int. J. Remote Sens.* **26**, 4485, (2005).

Supporting online material S2

The scaling of FPAR (IB-case)

In SiB2, fpar is derived from satellite observed normalized difference vegetation index and is vegetation type dependant. It varies between zero and one, with the value of one corresponding to a denser canopy. In the C, CV, and DR cases, FPAR is prescribed from satellite observations; it then affects the components of the surface energy, water and carbon balances but does not respond to them. In the DR-case, the assimilation rates calculated for each grid point of the C and CV-cases were averaged over the last 10 years of simulations and their ratios (gpp_C/gpp_CV) were applied directly to the maximum photosynthetic capacity V_{max} to reduce its values at every grid point and simulate a large down-regulation effect (1). In the IB case, we developed a method that allows FPAR to respond to changes in atmospheric CO_2 and the water availability generated by the

increase in CO_2 concentration. The method rests on the idea that in an increased atmospheric CO_2 concentration, terrestrial vegetation down regulates its physiological activity to save water resources but then grows more biomass to take advantage of the available CO_2 and the increased precipitation. The modeling consists in reducing the V_{max} but at the same time scaling up FPAR. Thus, at each grid point, the maximum photosynthetic capacity *vmax* was reduced by,

$$V\max new = V\max\{fpar\max * \frac{gpp\_C}{gpp\_CV} + (1 - fpar\max)\} \quad (1)$$

The ratios (gpp_CV/gpp_C) were applied to the IB-case, which incorporates down regulation; to increase proportionally FPAR. The scalar for FPAR was then obtained as:

$$scale = fpar\max * \frac{gpp\_CV}{gpp\_C} + (1 - fpar\max) * \frac{wstress\_C}{wtress\_CV} \quad (2)$$

Where *fparmax* is the maximum value for FPAR observed at each grid cell for the entire annual cycle; *wstress_CV* and *wstress_C* represent the water stress functions obtained in the CV and C cases, respectively. The water stress function is a measure of the water fraction in the model's root zone. It inhibits assimilation rates and conductance if the root zone's water level is low. The increase of fpar was modulated by the ratio of water stress between the C and CV runs (C/CV) to ensure that fpar is allowed to increase only over grid cells where water availability was not limiting evapotranspiration in the CV-

case. The first part of the right hand side of (eq. 2) compensates for the down-regulation, and the second part augments FPAR in the absence of water stress in the CV-case.

Finally scaled values of FPAR were obtained by multiplying the value of the original FPAR by the scaling function at each grid cell as:

$$fparnew = scale * fpar \tag{3}$$

The newly computed value *fparnew* was bound by a maximum allowable value *fpar_max_a,* as:

$$0.001 \leq fparnew \leq fpar\_\max\_a$$

(4)

Where *fpar_max_a* is obtained using *fparmax*, its corresponding value of maximum greenness fraction, *greenmax*, and the leaf area index maximum range corresponding to the grid cell's vegetation type, *zltmax*.

$$fpar\_\max\_a = 1.0 - e^{\frac{-park\max * zlt\max}{green\max}} \tag{5}$$

Using the new values of FPAR for all grid cells, global fields of vegetation cover fractions, leaf area index (LAI) and greenness fractions were obtained at all grid cells. These fields, along with the modified V_{max} fields were used as boundary conditions for the land surface model, SiB2, to run the IB-case forward.

The scaling procedure led to an overland average increase of about 25.3 % in FPAR and of 58.3 % in LAI. Over the Eastern regions of the United States illustrated in Fig.1, FPAR was increased by 24.3% and LAI by 54.8%.

References

1 P.J. Sellers et al, *Science*, **271**, 1402, (1996).